Letter | Editors' Suggestion | Featured in Physics

Amplitude of water pouring sound

Mouad Boudina [1,2], Joonoh Kim [1], and Ho-Young Kim [1,3,*]

[1]*Department of Mechanical Engineering, Seoul National University, Seoul 08826, Korea*

[2]*Department of Mechanical Engineering, University of British Columbia, Vancouver, British Columbia V6T 1Z4, Canada*

[3]*Institute of Advanced Machines and Design, Seoul National University, Seoul 08826, Korea*

(Received 5 May 2023; accepted 8 November 2023; published 21 December 2023)

We experimentally investigate the amplitude of the common sound heard when we pour water, tea, or coffee on a filled receptacle. Using water jets from circular nozzles, we find that pouring is audible when the nozzle distance from the free surface is above one-third of the jet breakup length. The sound amplitude increases with the steepness of the jet corrugation, informing that thin jets are louder than thick ones for a given pouring height. Since the jet corrugation is related to the air entrainment rate, the sound of pouring can serve as a practical noninvasive probe in aeration processes. After the jet breaks up into drops impacting on the free surface, the pouring sound amplitude increases with the nozzle diameter, unlike before breakup.

DOI: 10.1103/PhysRevFluids.8.L122002

The sound of liquid pouring, which we all hear almost everyday, has received growing attention in sensory marketing [1–3], for it can influence a consumer's perception of drinks. This supposedly mundane sound can play another potential role in cognitive therapy to assist stroke survivors in daily tasks such as preparing tea or coffee [4]. More applications involving liquid pouring currently drive a number of methods for realistic sound synthesis [5–7], which can be significantly improved once the physics of the phenomenon is uncovered. Whereas various investigations sought to understand water sounds in nature, e.g., streams [8], breaking waves [9,10] and rainfall in ocean [11], the acoustics of water pouring has scarcely been the subject of study thus far [12], therefore provoking our scientific curiosity.

A normal water pouring from a commercial plastic bottle is shown in Fig. 1(a). The jet has a nonuniform cross section yet a smooth and steady boundary. The jet penetration leaves, thus, the water free surface undisturbed and the pouring is silent. Water poured from a teapot, however, destabilizes early because of the spout roughness and orifice geometry [Fig. 1(b)]. The jet penetrates the free surface in a corrugated state, sometimes after breakup, and the pouring is audible even for the same pouring height as in the water bottle example.

This evidence questions a common misconception that the higher the jet the louder the sound, or that serving tea from a low distance avoids noise. We propose that jet corrugation is the main clue to the pouring sound amplitude. It depends, of course, on the jet height, but also on the orifice and the flow prior to plunging. This property bridges the water acoustics and jet dynamics so intensively studied [13,14].

The present Letter explores the origin and amplitude of the sound heard when we pour an inviscid liquid onto a pool, with regard to the jet diameter and length in particular. We consider a model water pouring, shown in Fig. 1(c), using smooth brass tubes of inner diameter d and aspect ratio of 20.

*hyk@snu.ac.kr

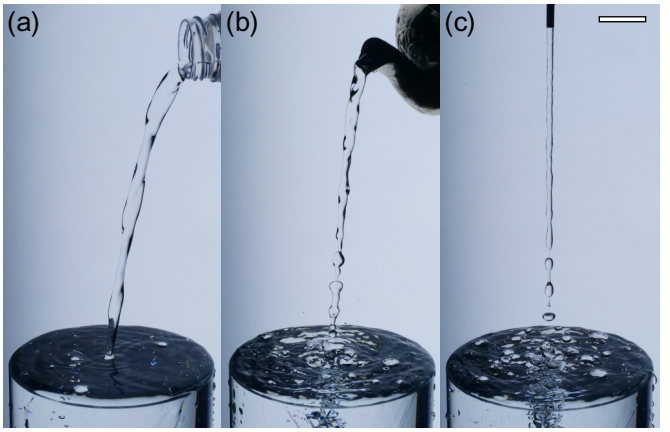

FIG. 1. Water pouring on a filled cylindrical cup from (a) a commercial plastic bottle and (b) a teapot. (c) Model water pouring from a smooth brass tube. Scale bar: 2 cm.

A water tank stands on a movable stage to change the nozzle distance l from the free surface and supplies the flow via gravity [Fig. 2(a)]. The tank diameter D_t is two orders of magnitude larger than the nozzle diameter, allowing us to assume a constant jet speed u_0 for each experimental trial. We pour water on a liquid-filled acrylic cylinder having larger dimensions ($D_c = 10$ cm, $H_c = 10$ cm) than the bubble penetration depth and width to avoid confining the plume of bubbles. A hydrophone (Teledyne Reson TC 4034) is placed $R_h \approx 3$ cm away from the jet impact without altering the bubble plume shape. The sound signal is amplified, filtered, and recorded for 10 s by a digital oscilloscope (Agilent Infiniium) with a sampling rate of 5 kHz.

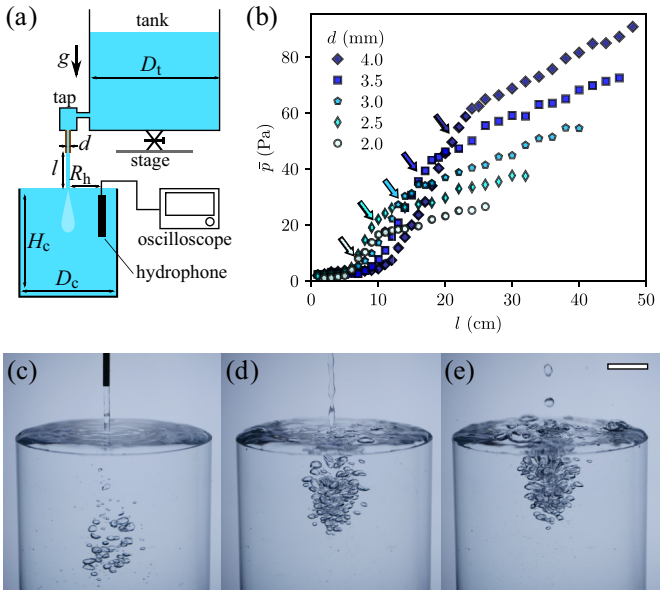

FIG. 2. (a) Experimental setup. The nozzle diameter is much smaller than the cup and tank diameters, $d \ll D_c < D_t$. (b) Pressure RMS $\bar{p}$ versus the nozzle distance l. Jet breakup occurs at the points indicated by arrows of corresponding color. (c)–(e) Images of plunging jet and bubble plume for $d = 3$ mm at $l = 3$, 10, and 25 cm, respectively. The breakup length is $l_B = 13.3$ cm. Scale bar: 2 cm. Note that the penetration depth of the bubbles decreases with the jet length and reaches a plateau.

TABLE I. Nozzle diameters d and jet speeds u_0 used in the experiments, with the corresponding jet breakup lengths l_B and corrugation wavelengths λ.

d (mm)	u_0 (m/s)	l_B (cm)	λ (cm)
2.0	2.3	6.9	0.8
2.5	2.3	9.8	1.1
3.0	2.4	13.3	1.3
3.5	2.4	16.4	1.5
4.0	2.4	21.7	1.7

Figure 2(b) shows the root mean square (RMS) of the pressure signal $\bar{p}$ against the nozzle distance l, obtained from the oscilloscope and collected for jet speeds and nozzle diameters listed in Table I. For short distances, the jet impacts on the free surface without noticeable disturbances and entrains a few bubbles that remain sparse in the liquid [Fig. 2(c)]. The pressure signal of the underwater sound is barely distinct from the ambient noise. As l increases, the jet corrugates and entrains more bubbles having a shorter penetration depth [15] [Fig. 2(d)]. The produced sound in this case is loud enough to be heard by human ear and detected by the hydrophone. When the jet breaks up due to the capillary instability, a train of drops impacts on the free surface and generates a pouring sound of a greater amplitude [Fig. 2(e)]. The curves $\bar{p}$ versus l all share the same profile regardless of the nozzle diameter, starting from the ambient noise level $\bar{p}_{\text{noise}}$ for short jets, then steeply increasing until breakup and slowly increasing beyond.

One of the main sound sources is the creation of an air volume in the liquid medium [16]. A single falling drop, for instance, forms a crater after impact that first expands, then collapses, and eventually releases a small bubble [17], marking exactly the onset of the plink sound [18]. On the other hand, a smooth jet carrying a bulge slightly bigger than the jet diameter is sufficient to compress the water surface and create an air cavity [19]. For a succession of bulges, as in our case, every crest creates a hollow cavity that pinches off from the interface and acoustically excites the bubbly mixture. A corrugated jet, therefore, triggers a series of pulses feeding the medium with energy and producing an uninterrupted pouring sound.

The force generated by a crest impact can be estimated as the product of the impulse pressure and the impact area. As schematized in Fig. 3(a), the latter scales as the surface covered by a single crest, $\pi[d^2/4 - (d/2 - \epsilon)^2] \approx \pi d\epsilon$. Here ϵ is the corrugation defined as the average size of troughs along the jet [20]. Since the water hammer effect induces the initial impulse of a falling drop on a free surface [21], we approximate the impulse pressure of the corrugated jet as $\rho c u_0$, where c is the sound speed and ρ the liquid density. At the hydrophone position, the pulse of magnitude $\sim\pi\rho c u_0 d\epsilon$ results in an acoustic force of $\sim\bar{p}R_h^2$, suggesting a direct proportionality of the pouring sound amplitude and the air entrainment rate defined as $Q_{\text{air}} \approx \pi u_0 d\epsilon$ [22].

To examine the relation between $\bar{p}$ and Q_{air}, we first extract the jet properties sketched in Fig. 3(a) using the image analysis tools detailed in Ref. [20]. We determine the breakup length l_B as the averaged position of the first unambiguous separation from the bulk. Then we calculate the characteristic wavelength of the corrugation λ as the value maximizing the averaged spatial spectrum of the jet boundary. As shown in Fig. 3(b), ϵ increases with l in a manner reminiscent of $\bar{p}$ versus l. Moreover, the ratio ϵ/λ, which represents the steepness of corrugation, is found to depend solely on l/l_B [Fig. 3(c)]. The corrugation steepness is hence self-similar and can be written as

$$\frac{\epsilon}{\lambda} = \mathcal{S}\left(\frac{l}{l_B}\right). \tag{1}$$

We note that the corrugation at the nozzle exit is nonzero owing to the boundary layer inside the nozzle [22]. This corrugation can still entrain air bubbles and generate pressure waves but is insufficient to exceed the ambient noise level.

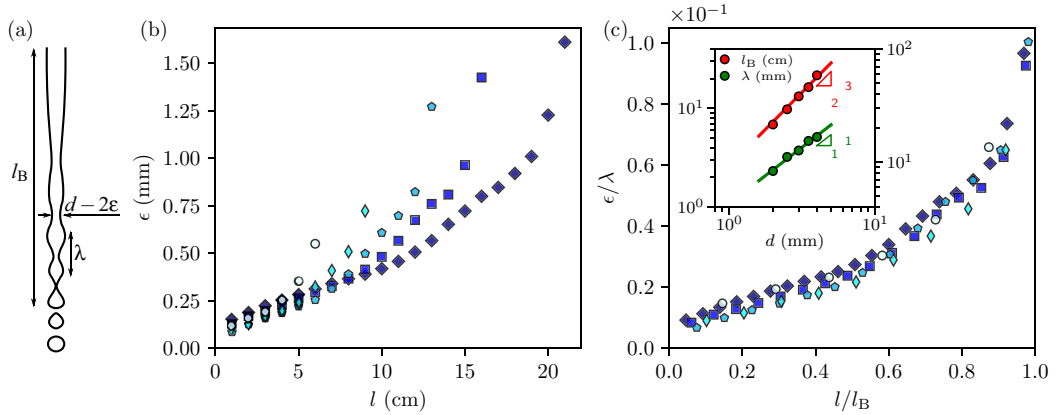

FIG. 3. (a) Schematics of an unstable jet, depicting the breakup length l_B, the wavelength λ, and the corrugation ϵ. (b) Corrugation versus nozzle distance. (c) Corrugation steepness ϵ/λ versus l/l_B. Inset: Breakup length (●, left y axis) and characteristic wavelength (●, right y axis) versus the jet diameter d. The red line is $l_B \propto 2.59 d^{3/2}$, and the green line is $\lambda \sim 4.27 d$, the latter prefactor being close to the theoretical value 4.51 [23].

The inset of Fig. 4 shows the pressure RMS versus the air entrainment rate. For low rates, we have $\bar{p} \sim \bar{p}_{\text{noise}}$, then $\bar{p} \propto Q_{\text{air}}$ after a detection threshold. Using Eq. (1) and $\lambda \sim d$ as in a varicose jet breakup [23] [inset of Fig. 3(c)], we write $Q_{\text{air}} \sim u_0 d^2 \mathcal{S}(l/l_B)$. Producing a detectable sound $\bar{p} - \bar{p}_{\text{noise}} > 0$ implies, therefore, that the jet impacts on the free surface with a sufficiently steep corrugation $\mathcal{S}(l/l_B) > \alpha$. By taking $\bar{p}_{\text{noise}} = \bar{p}|_{l/l_B \to 0}$, we find that the following relation for the

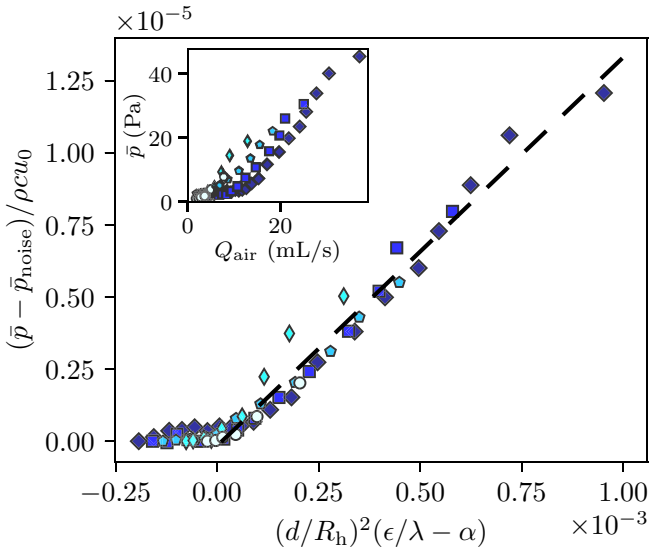

FIG. 4. Normalized pressure $(\bar{p} - \bar{p}_{\text{noise}})/\rho c u_0$ versus $(d/R_h)^2(\epsilon/\lambda - \alpha)$ before jet breakup ($l < l_B$). The dashed line is Eq. (2), and has a slope of $k = 1.35 \times 10^{-2}$ ($r^2 = 0.97$) for a detection threshold of $\alpha = 0.02$. Inset: Pressure RMS versus air entrainment rate $Q_{\text{air}} = \pi u_0 d \epsilon$.

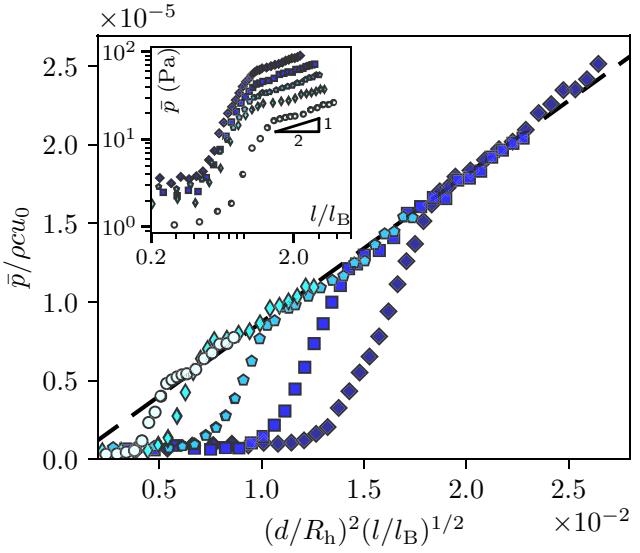

FIG. 5. Normalized pressure $\bar{p}/\rho c u_0$ versus the product $(d/R_\mathrm{h})^2(l/l_\mathrm{B})^{1/2}$. The dashed line is Eq. (4), which fits the data beyond break-up $l > l_\mathrm{B}$ ($r^2 = 0.99$). Inset: $\bar{p}$ versus l/l_B in logarithmic scale.

normalized pressure,

$$\frac{\bar{p} - \bar{p}_\mathrm{noise}}{\rho c u_0} \sim \left(\frac{d}{R_\mathrm{h}}\right)^2 \left[\mathcal{S}\left(\frac{l}{l_\mathrm{B}}\right) - \alpha\right] \text{ for } l < l_\mathrm{B}, \tag{2}$$

collapses the experimental data for $\alpha \approx 0.02$ (Fig. 4). Graphically from Fig. 3(c), the onset condition $\mathcal{S}(l/l_\mathrm{B}) > 0.02$ corresponds to $l/l_\mathrm{B} \gtrsim 1/3$.

Sound that can be heard by human ear needs to exceed a level above ambient noise $\bar{p} - \bar{p}_\mathrm{noise} > \Delta p^*$, which means that the ratio of the nozzle distance to breakup length should be greater than

$$\left(\frac{l}{l_\mathrm{B}}\right)^* = \mathcal{S}^{-1}\left(\alpha + \frac{\Delta p^* R_\mathrm{h}^2}{k \rho c u_0 d^2}\right), \tag{3}$$

with k the proportionality constant in Eq. (2) and $\mathcal{S}^{-1}$ the inverse of $\mathcal{S}$. Since $\mathcal{S}$ and $\mathcal{S}^{-1}$ are monotonically increasing functions, Eq. (3) reveals that $(l/l_\mathrm{B})^*$ increases as d and u_0 decrease. In other words, thin and slow jets can produce audible pouring only when close to breakup and the corrugation is important, whereas thick and fast jets can produce audible pouring well before breakup while carrying low corrugation.

It is worth mentioning that because the function $\mathcal{S} - \alpha$ increases faster than the cube of l/l_B (Fig. S3) and $l_\mathrm{B} \propto d^{3/2}$ [inset of Fig. 3(c)], the pressure RMS decreases with the nozzle diameter for a fixed $l < l_\mathrm{B}$ according to Eq. (2), consistent with the experimental data in Fig. 2(b). Said differently, thin jets are louder than thick ones for the same pouring height, inasmuch as the jet is continuous.

Now we consider the pouring sound when the nozzle distance l exceeds l_B, so the jet is broken into drops before hitting the free surface. We start from the empirically found dependency $\bar{p} \propto (l/l_\mathrm{B})^{1/2}$ as shown in the inset of Fig. 5, while the magnitude increases with the nozzle diameter d. We let $\bar{p} \sim A d^\beta (l/l_\mathrm{B})^{1/2}$, and take the limit to the breakup length, $\bar{p}B \sim A d^\beta$. Recalling from Eq. (2) for the continuous jet case that $\bar{p}B \sim \rho c u_0 (d/R_\mathrm{h})^2 [\mathcal{S}(1) - \alpha]$ at breakup, we find that $\beta = 2$ and

$A \sim \rho c u_0[\mathcal{S}(1) - \alpha]/R_h^2$. Therefore, we write

$$\frac{\bar{p}}{\rho c u_0} \sim \left(\frac{d}{R_h}\right)^2 \left(\frac{l}{l_B}\right)^{1/2} \text{for } l > l_B. \tag{4}$$

We find Eq. (4) to collapse all the postbreakup pressure measurements onto a single line as shown in Fig. 5. Using $l_B \propto d^{3/2}$ for a varicose breakup (inset of Fig. 3(c), we get $\bar{p} \propto d^{5/4} l^{1/2}$, i.e., the amplitude increases with the nozzle diameter unlike in the continuous jet regime.

A single drop entrains air and produces sound for specific sizes and impact velocities [11]. A train of drops, nonetheless, can entrain air even outside these conditions if they are sufficiently close to each other, such that the incoming drop impacts on the deformed surface before it recovers [24]. This condition reads as the time between impacts $\sim \lambda/u_0$ being shorter than the recovery time of the water interface $\sim (\rho d^3/\gamma)^{1/2}$, i.e.,

$$\frac{\rho u_0^2 d}{\gamma} > \left(\frac{\lambda}{d}\right)^2 \sim 20, \tag{5}$$

in view of $\lambda \sim 4d$ [inset of Fig. 3(c)]. The left-hand side of inequality Eq. (5) is the Weber number of the jet, and ranges from 140 to 320 in our experiments. If this condition is unfulfilled, the drop train would produce discrete plink sounds like in a slowly dripping faucet or no sound at all if the diameter and speed are outside the entrainment domain.

Although the passage of jet crests triggers the pouring sound, other plausible sources might be involved. First, the jet sends along the interface capillary ripples which fade away after a few jet diameters. These ripples have so small an amplitude and momentum that they leave the surface unaffected, and hence cannot be a main source of sound. Furthermore, the ascending bubbles gently touch the interface without causing vibration. Finally, once an ascending bubble arrives at the interface, it floats for a few seconds and bursts. The pressure waves produced as a consequence are, however, weakly radiated in water [25].

The effect of surface tension on the sound amplitude is implicitly considered via the breakup length in Eq. (2). Decreasing the surface tension, e.g., by warming the liquid or adding a surfactant, stabilizes the jet surface and delays breakup. Thus, the jet impinges on the free surface in a smoother state and gives a quiet pouring. If the water jet is turbulent or biphasic, as in a fully open faucet, the sound amplitude would be determined by a compound effect of turbulence, void fraction inside the jet, and the jet corrugation.

In summary, we carried out experiments to explore the relation between the amplitude of the pouring sound and the jet properties. The pouring is silent until the nozzle distance from the free surface is above one-third of the breakup length. Then, the sound amplitude increases with the steepness of the jet corrugation, itself related to the air entrainment rate. This result places the pouring sound as a potential noninvasive probe in water aeration applications, adding to the list of acoustic sensors, like in capillary flows [26]. After the jet breaks up, the drop train impacting on the free surface produces the familiar pouring sound so long as the Weber number is above 20, and the amplitude becomes an increasing function of the nozzle diameter as opposed to before breakup.

A prospective examination would consider the effect of liquid viscosity and the extent to which the nature of the pouring sound changes. It would also be worthwhile to complement the present Letter with a study of the splashing sound on a shallow pool, like when starting to fill an empty cup. A further comprehension of the pouring sound warrants a frequency analysis of its pitch, an essential aspect of the phenomenon, which is under our investigation.

This work was supported by the National Research Foundation of Korea (Grants No. 2018-052541 and No. 2021-017476) via SNU SOFT Foundry. The administrative support from SNU Institute of Engineering Research is gratefully acknowledged. We thank Prof. K. Park for helpful discussions.

[1] P. A. Cabe and J. B. Pittenger, Human sensitivity to acoustic information from vessel filling, J. Exp. Psychol. Hum. Percept. Perform. **26**, 313 (2000).
[2] C. Velasco, R. Jones, S. King, and C. Spence, The sound of temperature: What information do pouring sounds convey concerning the temperature of a beverage, J. Sens. Stud. **28**, 335 (2013).
[3] H. Perfecto, K. Donnelly, and C. R. Critcher, Volume estimation through mental simulation, Psychol. Sci. **30**, 80 (2019).
[4] C. Baber, A. Khattab, M. Russell, J. Hermsdörfer, and A. Wing, Creating affording situations: Coaching through animate objects, Sensors **17**, 2308 (2017).
[5] W. Moss, H. Yeh, J.-M. Hong, M. C. Lin, and D. Manocha, Sounding liquids: Automatic sound synthesis from fluid simulation, ACM Trans. Graph. **29**, 21 (2010).
[6] T. R. Langlois, C. Zheng, and D. L. James, Toward animating water with complex acoustic bubbles, ACM Trans. Graph. **35**, 95 (2016).
[7] H. Cheng and S. Liu, Liquid-solid interaction sound synthesis, Graph. Models **103**, 101028 (2019).
[8] T. G. Leighton and A. J. Walton, An experimental study of the sound emitted from gas bubbles in a liquid, Eur. J. Phys. **8**, 98 (1987).
[9] M. R. Loewen and W. K. Melville, A model of the sound generated by breaking waves, J. Acoust. Soc. Am. **90**, 2075 (1991).
[10] G. B. Deane, Sound generation and air entrainment by breaking waves in the surf zone, J. Acoust. Soc. Am. **102**, 2671 (1997).
[11] H. C. Pumphrey, L. A. Crum, and L. Bjorno, Underwater sound produced by individual drop impacts and rainfall, J. Acoust. Soc. Am. **85**, 1518 (1989).
[12] T. R. Hahn, T. K. Berger, and M. J. Buckingham, Acoustic resonances in the bubble plume formed by a plunging water jet, Proc. R. Soc. London A **459**, 1751 (2003).
[13] A. K. Biń, Gas entrainment by plunging liquid jets, Chem. Eng. Sci. **48**, 3585 (1993).
[14] K. T. Kiger and J. H. Duncan, Air-entrainment mechanisms in plunging jets and breaking waves, Annu. Rev. Fluid Mech. **44**, 563 (2012).
[15] G. D. Suciu and O. Smigelschi, Size of the submerged biphasic region in plunging jet systems, Chem. Eng. Sci. **31**, 1217 (1976).
[16] A. P. Dowling and J. E. Ffowcs Williams, *Sound and Sources of Sound* (Ellis Horwood, Chichester, 1983).
[17] O. G. Engel, Crater depth in fluid impacts, J. App. Phys. **37**, 1798 (1966).
[18] S. Phillips, A. Agarwal, and P. Jordan, The sound produced by a dripping tap is driven by resonant oscillations of an entrapped air bubble, Sci. Rep. **8**, 9515 (2018).
[19] Y. Zhu, H. N. Oğuz, and A. Prosperetti, On the mechanism of air entrainment by liquid jets at a free surface, J. Fluid Mech. **404**, 151 (2000).
[20] See Supplemental Material at http://link.aps.org/supplemental/10.1103/PhysRevFluids.8.L122002 for more information about the image analysis and extraction of the jet characteristics.
[21] J. A. Nystuen, Rainfall measurements using underwater ambient noise, J. Acoust. Soc. Am. **79**, 972 (1986).
[22] H. N. Oguz, The role of surface disturbances in the entrainment of bubbles by a liquid jet, J. Fluid Mech. **372**, 189 (1998).
[23] M. J. McCarthy and N. A. Molloy, Review of stability of liquid jets and the influence of nozzle design, Chem. Eng. J. **7**, 1 (1974).
[24] A. G. Bick, W. D. Ristenpart, E. A. van Nierop, and H. A. Stone, Bubble formation via multidrop impacts, Phys. Fluids **22**, 042105 (2010).
[25] N. Q. Lu, H. N. Oguz, and A. Prosperetti, The oscillations of a small floating bubble, Phys. Fluids A **1**, 252 (1989).
[26] A. Bussonnière, A. Antkowiak, F. Ollivier, M. Baudoin, and R. Wunenburger, Acoustic sensing of forces driving fast capillary flows, Phys. Rev. Lett. **124**, 084502 (2020).